Multichannel tunneling in the Cs_2 0_g^- photoassociation spectrum

Mihaela Vatasescu,[1,2] Olivier Dulieu,[1] Claude Amiot,[1] Daniel Comparat,[1] Cyril Drag,[1] Viatcheslav Kokoouline,[1,3] Françoise Masnou-Seeuws,[1] and Pierre Pillet[1]

[1]*Laboratoire Aimé Cotton, CNRS, Bâtiment 505, Campus d'Orsay, 91405 Orsay, France*

[2]*Institute for Space Sciences, P.O. Box MG-36, R76900 Magurele-Bucarest, Romania*

[3]*The Institute of Physics, Saint-Petersburg State University, Saint-Petersburg 198904, Russia*

(Received 6 October 1999; published 3 March 2000)

Two features with large rotational structure, observed at detunings $\delta_1 = -2.14$ cm^{-1}, $\delta_2 = -6.15$ cm^{-1} in the cesium photoassociation spectrum, are interpreted as due to the combined effect of tunneling through the barrier of the double-well $0_g^-(6s+6p_{3/2})$ potential, and channel mixing in the inner-well region. A precise value of the height of the barrier is given. The levels affected by these effects are expected to decay into low vibrational levels of the lowest triplet state, thus producing ultracold molecules.

PACS number(s): 34.20.−b, 32.80.Pj, 33.20.−t, 33.80.Ps

I. INTRODUCTION

The formation of ultracold molecules in their lowest electronic triplet state $a\,^3\Sigma_u^+$ or in their ground electronic state $X\,^1\Sigma_g^+$ has been observed for the first time [1] through photoassociation of two free cold cesium atoms into $0_g^-(6s+6p_{3/2})$ or $1_u(6s+6p_{3/2})$ Cs_2 excited electronic states (hereafter referred to as 0_g^- and 1_u). For most alkali dimers, the radiative decay of the excited long-range molecules formed by photoassociation yields back a pair of atoms in their ground state. However, the inner classical turning points R_i for the vibrational motion in these Cs_2 0_g^- and 1_u states are located in the ''intermediate long range'' of internuclear distances, i.e., $R_i \approx (16-30)a_0$ (see Fig. 1 for 0_g^-). Due to the slow variation ($\approx R^{-3}$) of the potential curve in this range, the motion is gradually stopped, so that spontaneous emission towards the $X\,^1\Sigma_g^+$ or $a\,^3\Sigma_u^+$ states can take place during a long time interval at distances $R \approx R_i$. The range of R_i values coincides with the location of the outer turning point for the uppermost vibrational levels of the $X\,^1\Sigma_g^+$ or $a\,^3\Sigma_u^+$ potential curve (with R^{-6} asymptotic behavior). Franck-Condon transitions can therefore efficiently transfer population towards these bound levels, allowing the formation of long-lived molecules. These molecules, whereas translationally ultracold, are expected to be created in high lying vibrational levels.

The double-well structure of the $Cs_2(0_g^-)$ potential curve is illustrated in Fig. 1, displaying two wells separated by a potential barrier at distance $R_b \approx 15a_0$. The vibrational levels of the external well (hereafter referred to as the ''regular'' series) have been assigned from $v_{ext}=0$ up to $v_{ext}=132$ in the photoassociation spectrum [2], allowing the determination of the relevant part of the potential curve through a combined Rydberg-Klein-Rees (RKR) and ''near dissociation expansion'' (NDE) analysis. A good agreement has been found with *ab initio* calculations [3,4]. However, such analysis provides no information on the height of the barrier nor on the inner well.

In the present work, we interpret the presence in the photoassociation spectrum of two structures not involved in the regular series, as due to both *tunneling* of vibrational wave functions through the barrier, and *electronic channel mixing* due to radial coupling in the region of the inner well. An estimate for the height of the barrier is given, while the emphasis is put on the necessity to introduce short distance channel mixing to reproduce the observations. Finally we discuss the efficiency of ultracold molecule formation after spontaneous emission from the levels affected by the tunneling.

II. EXPERIMENTAL SPECTRA

The experimental procedure has already been described in Refs. [1,2]. Let us recall briefly that the formed ultracold molecules are ionized into Cs_2^+ ions using a pulsed resonant two-photon absorption. We present in Fig. 2 details of the Cs_2^+ ion spectrum as a function of the detuning δ of the photoassociation laser relative to the $6s(F=4)+6p_{3/2}(F'=5)$ dissociation limit. Two previously unassigned structures G_1, G_2, that are not part of the ''regular'' series, are

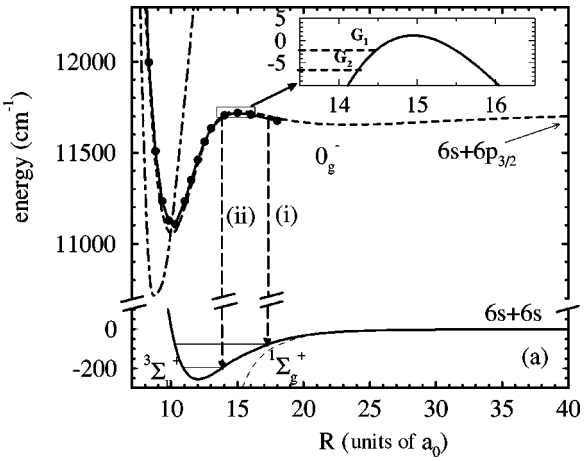

FIG. 1. Cs_2 molecular potential curves used in the present work. (a) $V_{6p}(R)$ [dashed line, not distinguishable from $V'_{6p}(R)$], $V_{6p}^{dia}(R)$ (solid line with circles), and $V_{5d}^{dia}(R)$ (dot-dashed line). Curves for the $X\,^1\Sigma_g^+$ and $a\,^3\Sigma_u^+$ triplet states are also displayed. The vertical lines (i) and (ii) schematize the spontaneous emission from the excited state when the vibrational motion takes place within the external or the internal well, respectively. (b) $V'_{6p}(R)$ in the region of the hump, with experimental binding energies of G_1 and G_2.

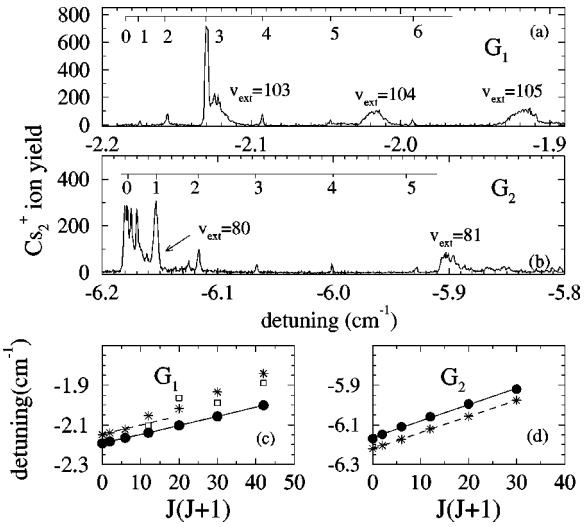

FIG. 2. Details of the photoassociation spectrum in the region of (a) the G_1 and (b) G_2 structures, with their J labeling. The rotational structure of the ''regular'' levels $v_{ext}=103,104,105$ is unresolved. (c) and (d) show the variation, as a function of $J(J+1)$, of the binding energies for the rotational levels identified in the G_1 and G_2 structures, and for the $n=163,J$ and $n=139,J$ levels of the coupled potentials. The slope of the curves yields the rotational constants. Black circles: experiment. Stars: computed energies for the $n=139,J$ and $n=163,J$ levels of the coupled potentials; open squares in (c): results for the $n=164$ level.

significantly more intense and display larger rotational structure than the neighboring ''regular'' lines. The structure G_1 displays rotational lines from $J_1=0$ to 6, and is located close to the $v_{ext}=103,104$ regular lines with unresolved rotational structure [Fig. 2(a)]. The $J_1=3$ line, at $\delta_1=-2.14$ cm^{-1}, on top of the $v_{ext}=103$ line, is about 7 times more intense. A rotational constant $B_v^1=137\pm4$ MHz has been fitted to the variation of the energies according to $E_v^1=B_v^1J(J+1)$ [Fig. 2(c)]. The structure G_2 is located close to $v_{ext}=80,81$, with a more intense component at $\delta_2=-6.15$ cm^{-1} on top of the $v_{ext}=80$ line [Fig. 2(b)]. The identification of the $J_2=0$ component is not easy as the G_2 structure is strongly embedded in the ill-resolved rotational structure of the $v_{ext}=80$ level. A rotational constant $B_v^2=243\pm8$ MHz can be extracted [Fig. 2(d)], once the position for the $J_2=0$ line is chosen as shown in Fig. 2(c).

From the definition of the rotational constant of a vibrational level v: $B_v=\langle\hbar^2/2\mu R^2\rangle_v$ ($\mu=121\,135.83au$ is the reduced mass for two cesium atoms), the mean value of the internuclear distance can be estimated according to $\overline{R}=\hbar/(2\mu B_v)^{-1/2}$. For G_1 and G_2 structures, respectively, this yields $\overline{R_1}\approx14a_0$ and $\overline{R_2}\approx12a_0$, which are typical values for vibrational motion in the region of the inner well of the 0_g^- curve. As in the photoassociation process the vibrational levels of the excited state are populated at large internuclear distances [5], it seems justified to assign the structures G_1 and G_2 to rovibrational levels of the inner well populated via tunneling through the barrier.

III. SINGLE-CHANNEL TUNNELING MODEL

First, we have studied the tunneling effect in the potential curve $V_{6p}(R)$ of the 0_g^- state obtained as follows [2]: starting from the two Hund's case *a*, *ab initio* curves of $^3\Sigma_g^+$ $(6s+6p)$ and $^3\Pi_g$ $(6s+6p)$ symmetry [3,4], matched to their asymptotic expansion [6], 0_g^- curves were derived by diagonalizing an R-independent effective fine structure Hamiltonian obtained from the atomic $6p$ doublet. The resulting $V_{6p}(R)$ upper 0_g^- curve (Fig. 1) has an inner well with a depth of 680 cm^{-1} and a minimum around $9.5a_0$, while the outer well has a depth of 78 cm^{-1} with a minimum at $R\approx25a_0$. The hump is found at $R=15a_0$ with a maximum lying 5 cm^{-1} below the $(6s+6p_{3/2})$ limit. This barrier is probably too low by a few wave numbers: indeed, apart from G_1 and G_2, all the lines in the observed spectrum [2] up to $\delta=-2$ cm^{-1} have small enough rotational constants to be assigned to vibrational motion restricted to the outer well. There is no evidence for vibrational levels lying above the barrier, with a wave function extending within both wells. Then we define a new curve $V'_{6p}(R)$ (inset of Fig. 1) by raising the hump of $V_{6p}(R)$ up to 2 cm^{-1} *above* the dissociation limit (without moving the external well). Such a change is well inside the standard accuracy of *ab initio* calculations.

Binding energies $E_{v,J}$ and rotational constants $B_{v,J}=\langle\Psi_{v,J}^*|\hbar^2/(2\mu R^2)|\Psi_{v,J}\rangle$, where $\Psi_{v,J}$ are the radial wave functions, are computed for all the vibrational levels in the double-well potential $V'_{6p}(R)$, using the mapped Fourier grid Hamiltonian (MFGH) method recently developed by Kokoouline *et al.* [7]. Among the 33 levels found (for $J=0$) in the inner well, tunneling occurs only for the highest level, bound by 2 cm^{-1} and with a rotational constant close to B_v^1. Moreover, the two upper levels are separated by ≈8 cm^{-1}. No reasonable modification of the $V'_{6p}(R)$ curve restricted to the inner well yields a picture compatible with the observation, i.e., tunneling for two levels separated by about 4 cm^{-1}, and with rotational constants *both* close to B_v^1 and B_v^2.

IV. MULTICHANNEL TUNNELING MODEL

Alternatively, one should consider the possibility of channel mixing in the region of the inner well. Indeed, another set of Hund's case *c* adiabatic potential curves were computed in W. Meyer's group [3], involving a molecular R-dependent fine structure coupling: the $0_g^-(6s+6p_{3/2})$ and $0_g^-(6s+5d_{3/2})$ curves display an avoided crossing at $R\approx10a_0$. The vibrational motion in the inner well of the lower curve is therefore coupled via radial coupling with motion in the upper one. A simple Landau-Zener diabatization procedure of these curves yields two diabatic potential curves $V_{6p}^{dia}(R)$ and $V_{5d}^{dia}(R)$ crossing at $R_c=10a_0$ (see Fig. 1), and a coupling matrix element estimated as $V_{6p,5d}^{dia}(R)=W\exp[-(R-R_c)^2/\Delta^2]$, where $W=56.6$ cm^{-1} and $\Delta=2a_0$ have been fitted to the adiabatic potential curves. This coupling reflects the mixing at short distances between the $(6s+6p)$ and $(6s+5d)$ configurations, leading to a nondiagonal term in

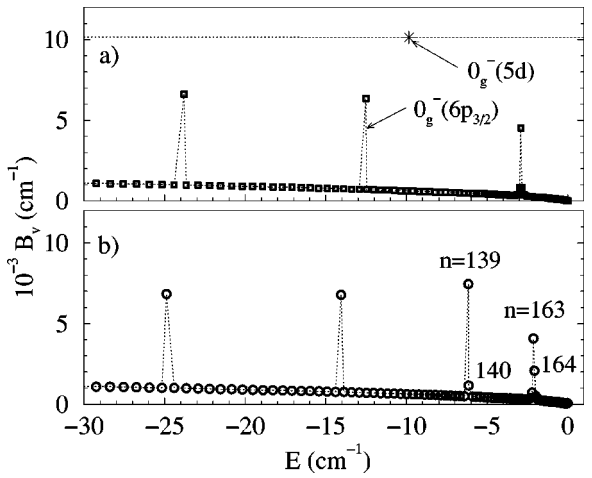

FIG. 3. Rotational constants for the vibrational levels of the V_{6p}^{dia} and V_{5d}^{dia} potentials. (a) uncoupled (b) coupled.

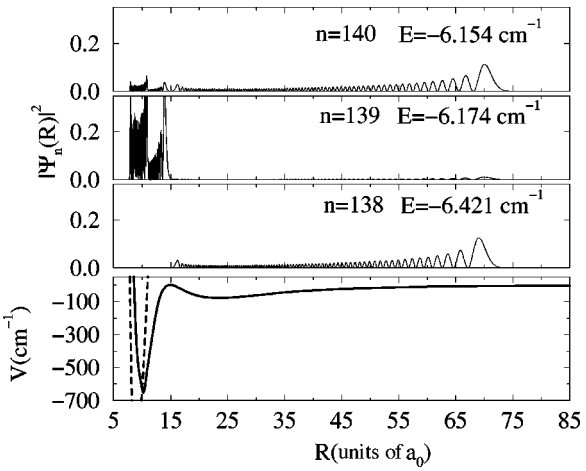

FIG. 4. Probability densities for the $n=138,139,140$ ($J=2$) levels of the coupled potentials V_{6p}^{dia} and V_{5d}^{dia}.

the effective spin-orbit Hamiltonian. While $V'_{6p}(R)$ and $V_{6p}^{dia}(R)$ are almost identical for $R>10.5a_0$, the top of the hump in $V_{6p}^{dia}(R)$ lies 1 cm^{-1} *below* $(6s+6p_{3/2})$, and the inner well, still located at $9.5a_0$, has a depth of 600 cm^{-1} only.

The energies $E_{v,J}$, wave functions $\Psi_{v,J}$, and rotational constants $B_{v,J}$ for the V_{6p}^{dia} and V_{5d}^{dia} coupled potentials are computed using the MFGH method. The introduction of a second channel now supplies two loosely bound vibrational levels in the inner-well region, close in energy, and both open to tunneling, in qualitative agreement with experiment. We have investigated the variation in their spacing obtained by slightly modifying the inner well in both $V_{6p}^{dia}(R)$ and $V_{5d}^{dia}(R)$, within the limits of an estimated accuracy for *ab initio* calculations of a few tens of cm^{-1}. Results in very good agreement with experiment are indeed obtained when the hump in $V_{6p}^{dia}(R)$ is made identical to the one in $V'_{6p}(R)$, the well depth being decreased by 40 cm^{-1}, while the curve $V_{5d}^{dia}(R)$ is lowered by 20 cm^{-1}. The resulting vibrational energies are displayed in Figs. 2(c) and 2(d) for the $n=163,164$ and $n=139$ levels of the coupled potential system. A comparison of the rotational constants obtained when turning off and on the coupling $V_{6p,5d}^{dia}$, is presented for $J=2$ in Figs. 3(a) and 3(b), respectively. In both cases, the narrow-spaced points with low $B_{v,2}$ values correspond to vibrational levels in the external well of V_{6p}^{dia}, behaving as a quasicontinuum when compared to levels in the inner wells. As discussed previously, the uncoupled calculations yield vibrational levels in the inner well of V_{6p}^{dia} (with $B_{v,2}\approx 200$ MHz) spaced by about 10 cm^{-1}, while a single level of V_{5d}^{dia} shows up in the present energy range. The slight reduction in the $B_{v,2}$ value of the last bound level in the V_{6p}^{dia} inner well manifests a small tunneling effect. In contrast, once the coupling is turned on, tunneling is clearly visible for the two last levels corresponding to vibrational motion mainly localized in the region of the inner wells and numbered $n=163$ and 139 [Fig. 3(b)]. The probability densities (see Fig. 4 for G_2) illustrate how the combined effect of tunneling and coupling in the inner well region may lead to important variations (up to one order of magnitude) in the rotational constants.

The computed rotational constants closely follow a linear variation with $J(J+1)$ for G_2 [Fig. 2(d)] with a 245 MHz slope, within the error bar of the experimental value $B_v^2=243\pm 8$ MHz. The agreement is still good for the G_1 structure, although the $J(J+1)$ variation in the computed $B_{v,J}$ constant is not strictly linear: several neighboring levels (as $n=163,164$) are now affected by the tunneling, which is extremely sensible to the shape of the top of the barrier, and varies by up to 12% from one J level to another. As the photoassociation probability depends upon the magnitude of the 0_g^- vibrational wave functions at the long range outer turning point [5,8,9], and then upon tunneling efficiency, such a J dependence could explain the marked differences in

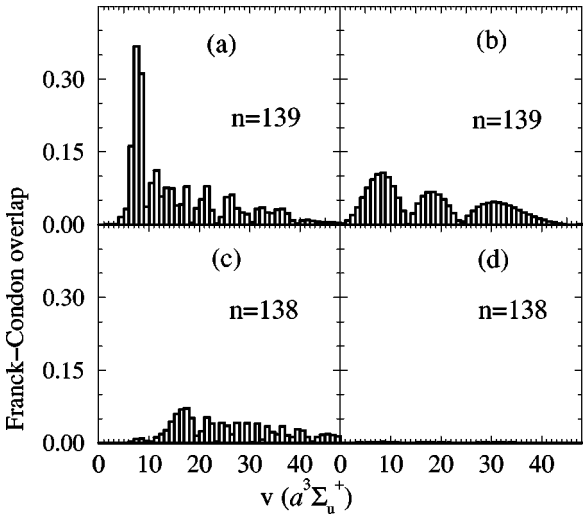

FIG. 5. Franck-Condon overlap of the vibrational functions of the $(n=139,J=2)$ and $(n=138,J=2)$ levels of the coupled potentials V_{6p}^{dia} and V_{5d}^{dia}, with the vibrational wave functions of the $(v,J=2)$ levels in the $a\,^3\Sigma_u^+$ ground state, as a function of v. (a) and (c): overlap with the component associated to the V_{6p}^{dia} potential; (b) and (d) overlap with the component associated to the V_{5d}^{dia} potential.

the intensities among the various components of G_1 and G_2 structures.

Finally, we have computed the overlap of both components of the two-channel vibrational wave functions for levels populated by tunneling with the wave functions for $a\,^3\Sigma_u^+$ vibrational levels (Fig. 5). It is clear that when tunneling is important, as in the case of the $n=139$ level, overlap with low vibrational levels in the ground state is markedly enhanced. More elaborate calculations should include the R dependence of the dipole moment and the modelization of the two-photon ionization process to provide quantitative results for the formation of the ultracold ground state molecules in *low-lying vibrational levels*.

As a conclusion, we have demonstrated that multichannel tunneling is a convincing explanation for the observation of two structures with large rotational constants and some relatively intense lines in the Cs_2 0_g^- $(6s+6p_{3/2})$ photoassociation spectrum. Reasonable modifications of the existing curves within their estimated accuracy lead to quantitative agreement between computed and experimental spectra, although no new information on the inner well of the potential curves can be extracted from these results. The height of the 0_g^- barrier can, however, be estimated as lying about 2 cm^{-1} above the $(6s+6p_{3/2})$ limit. The larger intensity of some lines suggests an increasing efficiency of the formation of cold molecules in low-lying vibrational levels of the lowest triplet potential curve, due to a short-range vibrational motion in the excited state enhanced by tunneling, in contrast with the usual photoassociation scheme. Future experiments should investigate the influence of the two-photon ionization scheme on the relative intensities in the spectra, and probe the formation of molecules that are ultracold for translational, vibrational, and rotational degrees of freedom. Complementary laser spectroscopy analysis of the inner wells are also required.

ACKNOWLEDGMENTS

M. Vatasescu acknowledges the financial support of the Romanian Government and World Bank under Grant No. CNSU 110, as well as a three-month grant from the Société de Secours des Amis des Sciences.

[1] A. Fioretti, D. Comparat, A. Crubellier, O. Dulieu, F. Masnou-Seeuws, and P. Pillet, Phys. Rev. Lett. **80**, 4402 (1998).
[2] A. Fioretti, D. Comparat, C. Drag, C. Amiot, O. Dulieu, F. Masnou-Seeuws, and P. Pillet, Eur. Phys. J. D **5**, 389 (1999).
[3] N. Spies, Ph.D thesis, Fachbereich Chemie, Universität Kaiserslautern, 1989 (unpublished).
[4] M. Foucrault, Ph. Millié, and J. P. Daudey, J. Chem. Phys. **96**, 1257 (1992).
[5] P. Pillet, A. Crubellier, A. Bleton, O. Dulieu, P. Nosbaum, I. Mourachko, and F. Masnou-Seeuws, J. Phys. B **30**, 2801 (1997).
[6] M. Marinescu and A. Dalgarno, Phys. Rev. A **52**, 311 (1995).
[7] V. Kokoouline, O. Dulieu, R. Kosloff, and F. Masnou-Seeuws, J. Chem. Phys. **110**, 9865 (1999).
[8] P.S. Julienne, J. Res. Natl. Inst. Stand. Technol. **101**, 487 (1996).
[9] R. Côté and A. Dalgarno, Phys. Rev. A **58**, 498 (1998).